

Date of current version 20 January 2023.

This work has been submitted to the IEEE for possible publication. Copyright may be transferred without notice, after which this version may no longer be accessible.

Digital Object Identifier XX.XXXX/ACCESS.2023.DOI

Machine Learning for Relaying Topology: Optimization of IoT Network with Energy Harvesting

KISEOP CHUNG¹ (Member, IEEE) and JIN-TAEK LIM² (Member, IEEE)

Agency for Defense Development, Daejeon 34186, Republic of Korea (e-mail: cks991030@snu.ac.kr¹, jtlim870708@gmail.com²)

Corresponding author: Jin-Taek Lim

This work was supported by the Agency for Defense Development Grant funded by the Korean Government(2023).

ABSTRACT

In this paper, we examine the internet of things system which is dedicated for smart cities, smart factory, and connected cars, etc. To support such systems in wide area with low power consumption, energy harvesting technology without wired charging infrastructure is one of the important issues for longevity of networks. In consideration of the fact that the position and amount of energy charged for each device might be unbalanced according to the distribution of nodes and energy sources, the problem of maximizing the minimum throughput among all nodes becomes a NP-hard challenging issue. To overcome this complexity, we propose a machine learning based relaying topology algorithm with a novel backward-pass rate assessment method to present proper learning direction and an iterative balancing time slot allocation algorithm which can utilize the node with sufficient energy as the relay. To validate the proposed scheme, we conducted simulations on the system model we established, thus confirm that the proposed scheme is stable and superior to conventional schemes.

INDEX TERMS unsupervised learning, variational autoencoder, IoT network, TDMA system, energy harvesting, relay.

I. INTRODUCTION

Internet of Things (IoT) technology could be considered to bring enormous innovations for societal and industrial systems in terms of improved efficiency, sustainability, and safety. With exchanging many types of information such as traffic, energy usage, and environment data (e.g., temperature, humidity), IoT devices can realize smart-city, connected industry, connected vehicles and integrated health care service [1]. Because these application services are expected to have numerous wireless devices with scalability and a long lifespan, the need for the easy-to-maintain wireless network which has a simplified topology is emerging. Also, in such a network, data being transmitted does not require high data rate but requires several different characteristics, such as frame sizes to be in the order of tens of bytes, intermittent transmission to be a few times per day, ultra-low speeds with an insensitive delay requirement, and mostly uplink-centric transmission. These requirements of an uplink-centric, low data rate and maintenance free network result in wireless-powered star-of-stars network technologies where a new air interface provides an energy-efficient relaying alternative to available wireless network systems, while covering larger areas.

Recently, a study on a relay-based star-of-stars topology for energy efficiency has been conducted to cover a large area [2]. In [2], they proposed a cooperative multi-hop transmission scheme in wireless sensor networks where the circuit energy consumption was taken into consideration and proved that the energy consumption per unit transmit distance can be minimized. As a new method for long-term operation without maintenance, researches on energy harvesting-based IoT networks are also being actively conducted [3]. In this energy harvesting-based IoT research area, there are some issues where the amount of energy charged by each node is different according to the distribution of the energy sources (e.g., power beacons (PBs)) and nodes, with the amount of residual/remaining energy in devices varying. In [4], they studied the resource allocation in energy harvesting (EH)-enabled Long range (LoRa) networks with the external energy sources such as power beacons. They solve the problem of regional energy distribution by the sub-optimal spreading factor and power allocation algorithm. Moreover, in [5], they proposed a clustering algorithm for grouping sensor nodes under consideration of energy distribution of the remaining nodes. These studies maximize the energy efficiency

of the network through scheduling under the distribution of energy. And, [6] proposed a distributed protocol maximizing the minimum sensing rate of sources operating in an energy harvesting-based IoT networks. They suggested the method for determining nodes to be charged, transmission power and charging duration of a PB, and routing of data by nodes and link scheduling. However, no prior works have considered the fact that, if the role of the node is not fixed, that is, if it is allowed to operate as a relay optimally adapting to the change of the energy distribution, energy efficiency could be more improved. To be specific, if certain node is close to PBs, it may have more harvested energy. Moreover, Nodes closer to the sink have the lower required energy for transmission, on the other side, nodes farther away from the sink have the higher required energy. Accordingly, if some nodes with sufficient energy can transmit data on behalf of nodes with lower energy, the efficiency of the entire network could be maximized.

However, this kind of routing problems are usually formulated as a max-min mixed integer optimization problem, which hinders solving optimal solution in polynomial time due to its NP-hardness and non-linearity of problem [7]. There may be several ways to overcome these complexities. In [8], they showed machine learning based techniques which is widely used in several nonlinear optimization problems. Recently, machine learning based techniques are also applied to various wireless network problems in [9]–[11]. The application of the machine learning for handling on graph-related problems was dealt in [12], based on supervised learning. However, it is difficult to solve this kind of problem with supervised learning because it is not an easy task to obtain labeled dataset due to its NP-hardness.

While in [13], variational autoencoder (VAE), first proposed by [14], could be considered as a way to solve the NP-hard problem in an semi-supervised manner. Especially, in [15], they implemented a chemical molecule graph generative model using a VAE, while its application was limited in smaller graphs only and a dataset for training was needed, which makes it difficult to apply it directly to the NP-hard problem.

Considering these facts, in this article, we propose a VAE-based scalable and unsupervised machine-learning scheme that can determine the dynamic relay topology under the regional distribution of nodes and energy, along with our novel backward-pass based rate evaluation method, called "Packet-Tracing"(PT) in this paper, which can properly and concisely assess the output of our VAE scheme and thus gives a proper direction for training the VAE scheme. Moreover, we proposed an iterative balancing (IB) algorithm for time slot allocation over a time-division multiplexing access (TDMA) based system, which finally gives the solution on both topology planning and time slot planning for the formulated max-min optimization problem.

The remainder of this paper consists of follows: In Section II, we define our system model and formulate a max-min optimization problem, our problem to solve. In Section III, from the problem formulation, we present a topology algorithm based on variational autoencoder method and a time slot allocation algorithm that maximizes the max-min fairness of nodes under a TDMA system. In Section IV, we present operation details of our proposed scheme and perform numerical simulations and

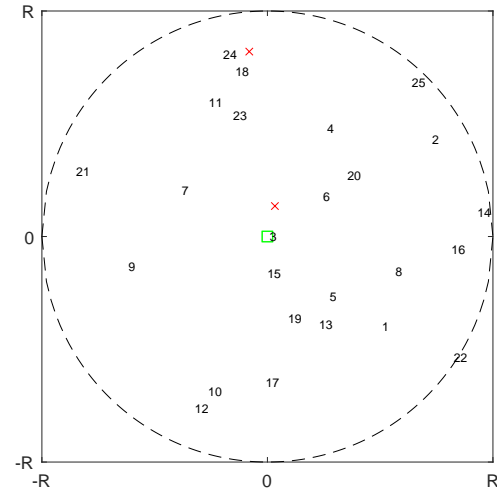


FIGURE 1. Network example (number : IoT Nodes, \times : Power Beacons, \square : Sink) analysis which confirm sub-optimality of our proposed scheme, leading to our conclusions in Section V.

II. SYSTEM MODEL AND PROBLEM FORMULATION

In this section, we describe the system model. We consider the uplink transmissions in an IoT sensor network during the time frame T . In our system model consideration, N_d IoT devices (shortly, nodes) are uniformly distributed in a circle of radius R centred around the sink. Let us denote $\mathbb{N}_d = \{1, 2, \dots, N_d\}$ as the set associated with nodes. By indexing the packet sink with $N_d + 1$, we can define $\mathbb{N} = \mathbb{N}_d \cup \{N_d + 1\}$ as the communicating node set. In addition, a TDMA system is assumed in our system model. TDMA is an effective system to alleviate the performance of nodes which placed in inferior power/position environment [16], by allocating more time slots within uplink frame by taking spare time slots from the nodes which placed in superior power/position environment. The considered time frame T is divided into N_d time slots and allocated to each IoT device, whose time slot for each node n is indicated by $t_n \in (0, T)$. During t_n , node n has the opportunity to transmit.

Next, we consider energy harvesting (EH) for our system model. In our model, each node is self-powered by harvesting energy from PBs and stores the remaining energy in a rechargeable battery with limited capacity. Power beacons(PB) of energy can be of any type (solar or RF or others), and only one condition applies if RF source is considered, whose frequency band should be different from the communication band is used. This condition is considered to alleviate the possibility that the energy harvesting signals cause additional interference to sink. In our problem, PBs are also randomly located in the cell with radius R , whose transmit power is defined as P_b . Let us denote $\mathbb{N}_b = \{1, 2, \dots, N_b\}$ as the set associated with PBs. An example of the network is presented in Fig. 1, consisting of 2 PBs, and 25 nodes around the sink.

In this configuration, the harvested energy of node n which is sent from the PBs can be defined as

$$E_{rec,n} = T \sum_{i \in \mathbb{N}_b} P_b |h_{i,n}|^2 d_{i,n}^{-\alpha} \quad (1)$$

where $d_{i,n}$ is the distance between node i and node n , $h_{i,n}$ is the channel between node i and node n which follows a complex Gaussian distribution with zero-mean and unit variance, such

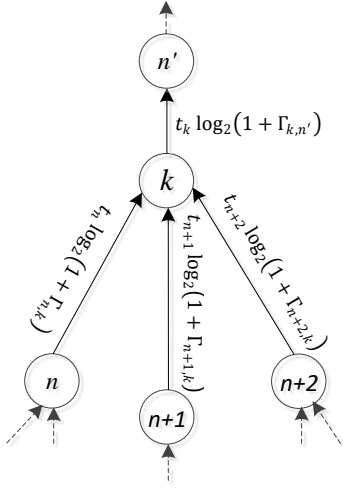


FIGURE 2. Illustration of relaying data from lower nodes to higher node

that $h_{i,n} \sim \mathcal{CN}(0, 1)$ and α is the path-loss exponent. In our system model, we consider a discrete time block-fading model, where the channel state is constant for a time frame T [17], and also assume that the instantaneous channel state information for $h_{i,n}$ is available.

Then, the harvested energy at each node depends on which EH model is considered either linear or nonlinear [18]. One of the nonlinear EH models could be considered is a sigmoidal model [4], which was shown to fit well with the experimental result. In this paper, the linear model is considered for simplicity, but the nonlinear models can also be applied. When the linear model is considered, the harvested energy E_n is given by $E_n = \eta E_{rec,n}$, where $\eta \in [0, 1]$ is the conversion efficiency.

We also assume that the harvested energy during T is consumed for signal transmission in t_n time slot in the next T time window, where $\mathbf{t} = \{t_n | \forall n \in \mathbb{N}_d\}$. Then, the transmit power could be expressed as $P_n = \frac{E_n}{t_n}$.¹ In addition, in the TDMA system, the signal-to-noise ratio from a transmitting node n to a receiving node n' , $\Gamma_{n,n'}$, can be expressed as $\Gamma_{n,n'} = \frac{P_n |h_{n,n'}|^2 d_{n,n'}^{-\alpha}}{N}$ where N is the noise power.

Moreover, we define $\mathbf{c} = \{c_{n,n'} | \forall n \in \mathbb{N}_d, \forall n' \in \mathbb{N}\}$ whose element is $c_{n,n'} \in \{0, 1\}$ to represent the connection of the relay topology where $c_{n,n'} = 1$ if node n transmits its data and children's data to node n' , otherwise $c_{n,n'} = 0$. Using the definition of \mathbf{c} and Shannon's capacity, the amount of bits per frequency (bits/Hz) that node k could transmit is defined as $\sum_{n' \in \mathbb{N}, n' \neq k} c_{k,n'} t_k \log_2(1 + \Gamma_{k,n'})$, and the amount of bits per frequency (bits/Hz) that node k receives is expressed as $\sum_{n \in \mathbb{N}_d, n \neq k} c_{n,k} t_n \log_2(1 + \Gamma_{n,k})$ (as shown in Fig. 2). Then, the difference between the two amount could be considered as the amount of bits per frequency (bits/Hz) the node k itself can transmit, denoted as $B_k(\mathbf{c}, \mathbf{t})$, could be expressed as follows:

$$B_k(\mathbf{c}, \mathbf{t}) = \sum_{n' \in \mathbb{N}} c_{k,n'} t_k \log_2(1 + \Gamma_{k,n'}) - \sum_{n \in \mathbb{N}_d, n \neq k} c_{n,k} t_n \log_2(1 + \Gamma_{n,k}) \quad (2)$$

Therefore, the optimization problem for maximizing the minimum of B_k among all nodes, \mathbb{N}_d , could be formulated as follows.

$$(P1) \quad \max_{\mathbf{c}, \mathbf{t}} \min_k B_k(\mathbf{c}, \mathbf{t}) \quad (3)$$

$$\text{s.t.} \quad \frac{1}{T} \sum_{n \in \mathbb{N}_d} t_n = 1, \quad (4)$$

$$\sum_{n' \in \mathbb{N}} C_{n,n'} = 1, \quad \forall n \in \mathbb{N}_d, \quad (5)$$

$$(\mathbf{C}^{N_d})_{n, N_d+1} = 1, \quad \forall n \in \mathbb{N}_d \quad (6)$$

where \mathbf{C} is the extended adjacency matrix of topology, whose $C_{n,n'} \in \{0, 1\}$, $\forall n \in \mathbb{N}_d, \forall n' \in \mathbb{N}$, $C_{N_d+1,n} = 0$, $\forall n \in \mathbb{N}_d$ and $C_{N_d+1, N_d+1} = 1$. (4) guarantees that the sum of t_n for all nodes is T . (5) indicates that each node's outward link is only connected to one of the other nodes including the sink. (6) means that every node is connected to the sink in the end.²

This optimization problem is NP-hard so an exact algorithm demands the enormous computational effort. However, by decoupling the problem into two sub-problems, we can transform the original problem with \mathbf{c} and \mathbf{t} to the single variable problem with \mathbf{c} .

For a given \mathbf{c} , the problem (P1) can be transformed to

$$(P1-1) \quad \max_{\mathbf{t}} \min_k B_k(\mathbf{c}, \mathbf{t}) \quad (7)$$

$$\text{s.t.} \quad \frac{1}{T} \sum_{n \in \mathbb{N}_d} t_n = 1. \quad (8)$$

since we can always find \mathbf{t} satisfying (P1-1) by using the IB time slot allocation algorithm which is proposed in the next section, by satisfying $\max_k B_k(\mathbf{c}, \mathbf{t}) = \min_k B_k(\mathbf{c}, \mathbf{t})$ under the given \mathbf{c} . In other words, \mathbf{t} could be considered as a variable determined by \mathbf{c} . If we define the optimal value of (P1-1) as $B_{IB}(\mathbf{c})$, the original problem (P1) could be expressed as below:

$$(P1-2) \quad \max_{\mathbf{c}} B_{IB}(\mathbf{c}) \quad (9)$$

$$\text{s.t.} \quad \sum_{n' \in \mathbb{N}} C_{n,n'} = 1, \quad \forall n \in \mathbb{N}_d, \quad (10)$$

$$(\mathbf{C}^{N_d})_{n, N_d+1} = 1, \quad \forall n \in \mathbb{N}_d. \quad (11)$$

Besides, we can ignore the constraints (10) and (11) since \mathbf{c} not satisfying those constraints gives $B_{IB}(\mathbf{c}) \leq 0$. Unfortunately, for solving (9), no computationally efficient method could be applied without involving exhaustive search which has time complexity of at least $\mathcal{O}((N_d + 1)^{N_d-1})$. In order to avoid such time complexity limitation, we propose the variational

¹For simplicity, we assume that E_n is used only for the transmission, not for the transmission/reception electronic circuit [19]. For an accurate model, such as the first order radio model, the circuit power consumption should be taken into account, but it will only result in some difference in the degree of improvement of our proposal.

²According to the adjacency matrix \mathbf{A} , n -th matrix multiplication of adjacency matrix element $(\mathbf{A}^n)_{i,j}$ indicates whether there are n -hop path exists from node i to node j . Since adjacency matrix mentioned here has been extended to have a self-cycle at the packet sink, so that we include all m -hop path while regarding extended adjacency matrix multiplication $(\mathbf{A}^n)_{i,j}$ where $m \leq n$.

autoencoder(VAE) based Machine-Learning algorithm in the next section.

III. DESCRIPTION OF THE ALGORITHM

In this section, we propose a VAE scheme to find \mathbf{c}^* and our novel Packet-Tracing(PT) algorithm to assess the VAE scheme, along with iterative balancing(IB) time slot allocation to find \mathbf{t}^* , finally gives the sub-optimal solution over both \mathbf{c} and \mathbf{t} .

A. TIME SLOT ALLOCATION ALGORITHM

Algorithm 1 Iterative Balancing (IB) algorithm for \mathbf{t}^*

```

1:  $t_n = \frac{T}{N_d}, \forall n \in \mathbb{N}_d$ 
2:  $\delta_1 = \infty$ 
3: while  $\epsilon_1 < \delta_1$  do
4:    $i^* = \arg \max_k B_k(\mathbf{c}, \mathbf{t}), j^* = \arg \min_k B_k(\mathbf{c}, \mathbf{t})$ 
5:    $\Delta = t_{i^*}$ 
6:    $\delta_2 = \delta_1$ 
7:   while  $\Delta > 2\epsilon_2$  &  $\epsilon_1 < |\delta_2|$  do
8:      $\Delta = \Delta/2$ 
9:     if  $\delta_2 > 0$  then
10:       $t_{i^*} = t_{i^*} - \Delta$ 
11:       $t_{j^*} = t_{j^*} + \Delta$ 
12:       $\delta_2 = B_{i^*}(\mathbf{c}, \mathbf{t}) - B_{j^*}(\mathbf{c}, \mathbf{t})$ 
13:     else
14:       $t_{i^*} = t_{i^*} + \Delta$ 
15:       $t_{j^*} = t_{j^*} - \Delta$ 
16:       $\delta_2 = B_{i^*}(\mathbf{c}, \mathbf{t}) - B_{j^*}(\mathbf{c}, \mathbf{t})$ 
17:     end if
18:   end while
19:    $B_{\max} = \max_k B_k(\mathbf{c}, \mathbf{t}), B_{\min} = \min_k B_k(\mathbf{c}, \mathbf{t})$ 
20:    $\delta_1 = B_{\max} - B_{\min}$ 
21: end while
22:  $B_{\text{IB}}(\mathbf{c}) = B_{\min}$ 

```

In this subsection, we propose iterative balancing (IB) time slot allocation algorithm, which derives the optimal \mathbf{t} satisfying (P1-1) under given \mathbf{c} , thus maximizes B_{\min} . Firstly, we defined hyper-parameter for the algorithm ϵ_1, ϵ_2 , which means the upper bound of the difference between B_{\max} and B_{\min} and the minimum allocatable time slot, respectively. Additionally, the condition $\epsilon_2 \ll T$ and $B_k(\mathbf{c}, 2\epsilon_2) < \epsilon_1$ for $\forall k \in \mathbb{N}_d$ must be met in order to guarantee the convergence of our algorithm.

The key principle of the proposed algorithm is to repeatedly reduce the difference between B_{\max} and B_{\min} . First, under the initial \mathbf{t} assignment, we find $i^* = \arg \max_k B_k(\mathbf{t})$ and $j^* = \arg \min_k B_k(\mathbf{t})$. Then, the bisection algorithm is repeatedly applied to make the amount of bits per frequency between the node i^* and j^* , δ_2 , less than ϵ_1 , or to make the remaining time slot of the node i^* except for its minimum allocatable time slot, $t_{i^*} - \epsilon_2$, less than ϵ_2 . Then the bisection algorithm sets $\Delta = \Delta/2$ and reduces the time slot of node i^* by Δ and instead allocates that reduced Δ to node j^* .

When the bisection algorithm of the two selected nodes is finished, the same procedure is repeated by obtaining newly founded node i^* and node j^* under condition depicted as above. This procedure is performed until $\delta_1 = B_{\max} - B_{\min}$ becomes

less than ϵ_1 . A detailed description of the process described is given in Alg. 1. Furthermore, the convergence proof of Alg. 1 is given as follows.

Proposition 1. *Let us define $B_{\max,k}$, $B_{\min,k}$ and $\delta_{1,k}$ as B_{\max} , B_{\min} and δ_1 in k -th iteration of outer loop which consists of line 3 to 21 in Alg. 1, respectively. Then, $\delta_{1,k} = (B_{\max,k} - B_{\min,k}) \leq \epsilon_1$ is satisfied for $\exists k$ in total outer loop iteration count domain.*

Proof. Let us define the time slot allocated to the node i and the amount of bits per frequency of node i at the beginning of the k -th iteration as $t_{i,k}$, and $B_{i,k} = B_i(t_{i,k})$, respectively. In this notation, $B_{\max,k}$ and $B_{\min,k}$ at the beginning of the k -th iteration could be written with $B_{i^*}(t_{i^*,k})$ and $B_{j^*}(t_{j^*,k})$, respectively.

On the other hand, the end of the inner loop consists of line 7 to 18 in Alg. 1 means that the condition $\Delta \leq 2\epsilon_2$ or the condition $\epsilon_1 \geq |\delta_2|$ has been met. If at least one iteration of the inner loop has been performed, we can find such proper positive constant σ among all outer loop iteration that satisfies $\sigma < \min(B_{\max,k} - B_{i^*,k+1}, B_{j^*,k} - B_{\min,k+1})$ and $\sigma < \epsilon_1$ according to lemma 1. Since $\Delta > \epsilon_2$ is always guaranteed, this fact eventually guarantees existence of constant σ and $N_\delta < N/2$ satisfying $\delta_{1,k} \geq \delta_{1,k+N_\delta} + \sigma$ for $\forall k$ in total outer loop iteration count domain.

Thus, in this case, the two expressions $\delta_{1,k} \geq \delta_{1,k+N_\delta} + \sigma$ and $\delta_{1,k} \geq 0$ are always satisfied for $\forall k$ and constant $\exists \sigma > 0$ and $\exists N_\delta < N/2$, eventually leads to the satisfaction of the condition $\delta_{1,k} \leq \epsilon_1$ for some k .

However, such termination condition of the inner loop could be met at the beginning of the inner loop iteration, hence the iteration of the inner loop may not be performed. Nevertheless, neither condition could not be met at the beginning of the first iteration of the inner loop.

Firstly, satisfying the former condition $\Delta \leq 2\epsilon_2$ means that $t_{i^*,k} \leq 2\epsilon_2$ since we set initial $\Delta = t_{i^*}$. Subsequently, the inequality $\delta_{1,k} \leq B_{i^*}(t_{i^*,k}) \leq B_{i^*}(2\epsilon_2) < \epsilon_1$ is justified since condition $B_i(\mathbf{c}, 2\epsilon_2) < \epsilon_1, \forall i \in \mathbb{N}_d$ is given. Next, satisfying the latter condition $\epsilon_1 \geq |\delta_2|$ implies that $\epsilon_1 \geq \delta_{1,k}$ has been met, since we set initial $\delta_2 = \delta_{1,k}$.

Therefore, it can be shown that both case already satisfies the termination condition of the outer loop, eventually satisfies the proposition. \square

Lemma 1. *There are always such a positive constant σ satisfying $\sigma < B_i(t_A) - B_i(t_B)$ and $\sigma < \epsilon_1$ for $\forall i \in \mathbb{N}_d$ exists while $B_n(t_n) = t_n \log_2(1 + \Gamma_{n,n'})$ is given with $\Gamma_{n,n'} = \frac{P_n |h_{n,n'}|^2 d_{n,n'}^{-\alpha}}{N}$ and $P_n = \frac{E_n}{t_n}$, respectively, and satisfies $\epsilon_2 \leq t_A - t_B$ and $c_{n,n'} = 1$.*

Proof. Let us denote $B_i(t) = t \log_2(1 + \frac{\tau_i}{t})$ for some constant τ_i since $E_n, |h_{n,n'}|^2, d_{n,n'}^{-\alpha}, N$ is constant. Next, we denote the node index i^* satisfies the condition $B_{i^*}(T + \epsilon_2) - B_{i^*}(T) \leq B_i(T + \epsilon_2) - B_i(T)$ for $\forall i \in \mathbb{N}_d$.

Note that function $B_i(t)$ is monotonic increasing function and $\frac{\partial^2}{\partial t^2} B_i(t) < 0$ in domain $t \in \mathbb{R}_+^+$. Then, the inequality $B_i(T + \epsilon_2) - B_i(T) < B_i(t_A) - B_i(t_B), \forall i \in \mathbb{N}_d$ is justified since condition (4) exists, restricting t in $0 < t < T$.

Also, since condition $B_i(\mathbf{c}, 2\epsilon_2) < \epsilon_1, \forall i \in \mathbb{N}_d$ is given, the inequality $B_{i^*}(T + \epsilon_2) - B_{i^*}(T) < B_{i^*}(\mathbf{c}, 2\epsilon_2) - B_{i^*}(\mathbf{c}, \epsilon_2) < B_{i^*}(\mathbf{c}, 2\epsilon_2) < \epsilon_1$ is justified.

Thus, it is sufficient to set positive constant σ satisfying the lemma above as $B_{i^*}(T + \epsilon_2) - B_{i^*}(T)$. \square

B. MACHINE LEARNING BASED TOPOLOGY ALGORITHM

In this subsection, we propose a machine-learning based VAE model and a backward-pass based rate evaluation model, called Packet-Tracing evaluation model (PT-EVM) in this paper, inspired by the ray tracing method which used in 3-D graphics rendering. Our proposed model to find \mathbf{c}^* consists of two parts, firstly derives \mathbf{c}^* using the VAE part, and assesses derived \mathbf{c}^* with the PT-EVM part, finally trains the VAE part with the assessment from the PT-EVM part.

Since (P1-2) has non-linearity and discontinuity characteristics due to the nature of the Shannon-capacity formula and the mixed-integer problem, it is challenging to find sub-optimal \mathbf{c}^* using analytical methods. Given these considerations, we propose machine-learning as a method to overcome these limitations. However, there are some restrictions to apply supervised-learning in our formulated problem, since dataset to be used for supervised learning, such as a pair set of positional distribution among nodes and PBs and optimal topology, is cannot be obtained due to the characteristics of our formulated problem. Moreover, it is difficult to build such dataset in an exhaustive search way due to the computation time growing exponentially with the number of nodes.

Taking these limitations into consideration, we propose the VAE based generative model which can be used in unsupervised learning manner. Typically, generative models are used to resemble observed dataset and embed dataset to high-dimensional space, called latent vector space, thus gain the ability to generate new data point based on observed distribution by simply modifying newly latent vector.

Considering this fact, our generative model and unsupervised-learning hybrid scheme slightly modifies those original structures, which explores latent vector space and its mapped data point space to derive sub-optimal solution \mathbf{c}^* . However, in order to realize the proposed concept depicted as above, a proper assessment over resulting output \mathbf{c} is necessary, which enables exploration of the latent vector space and derivation of the sub-optimal solution.

One may think an alternative solution as a reinforcement learning method which retrieves reward from interacting with a physical network, by applying resulting topology from algorithm to the physical network, then analyzes real achievable rate as reward for reinforcement learning. But there are some drawbacks. When model is in learning phase, model results imperfect topology output, which is essential procedure for receiving reward to use in the reinforcement learning, as a result initial performance degradation while learning in practical use is inevitable. Moreover, since depicted in Section I, IoT network environment has ultra-low speed intermittent transmission property, meaning that there are very low frequency of reward which can be used in reinforcement learning, thus maximizes the drawback depicted as above, finally resulting impropriety to apply reinforcement learning.

Therefore, simulation-based assessment for resulting topology is essential while it requires both brevity but sufficient detail to provide precision of network modeling. However, conventional network modeling and simulation (M&S) tool such as NS-3 or Riverbed Modeler requires excessive computing overhead since they simulates the whole network operation, such as buffer management, TCP/IP protocol procedure, wireless channel emulation and packet switching among interacting interfaces and so forth. Such simulation overhead is unnecessary since our assessment requirement is enough to examine achievable rate over nodes with regards to congestion and distribution of PBs and nodes. One imaginable solution is subtract the sum of inbound capacity from the sum of outbound capacity on the basis of the definition of Shannon's capacity, depicted as (2). Unfortunately, this naive solution cannot consider about how much of rate(packet) will be inbound to specific node and how much of rate(packet) could be handled in destination node regarding congestion.

Since those limitations and requirements cannot be fully reflected through typical solutions, we propose packet tracing (PT) algorithm to enable congestion-aware rate assessment. In PT algorithm, we sequentially assign node's achievable rate starting with packet sink and towards backward-pass manner, like ray-tracing algorithm in 3-D graphics rendering. Ray-tracing works by tracing a path from a viewpoint(camera) to object in virtual 3-D graphics space, and ray propagates under photonics simulation, eventually hits the light source, finally the ray is showing valid path to light to propagate [20]. Since ray-tracing algorithm does not take into account for rays which don't reach the camera, thus reducing the computation cost drastically. Similarly, in our packet-tracing algorithm, its backward-pass property provides both feasible and concise rate assessment similar to ray-tracing algorithm's.

As shown in Fig. 3, the proposed unsupervised-learning model consists in two parts, mainly VAE part and PT-EVM part. In a nutshell, such proposed concept could be implemented by entering a random latent vector input into VAE, assessing the output \mathbf{c} , and updating the parameters of VAE using these assessment iteratively. This procedure eventually focuses and maps prior latent vector space to sub-optimal solution data point and draws \mathbf{c}^* without the dataset necessary for supervised learning. Detailed description of each part of scheme is depicted subsections continuing below.

1) VAE structure

The VAE part functions as generating a topology for given latent vector input. The left side part of Fig. 3 depicts variational autoencoder structure, as 4 fully connected (FC) layers and 3 rectified linear unit (ReLU) layers between each fully connected layers, following by 2Dmap layer and softmax layer.

Firstly, in the fully connected layer, each input element x_i is processed into output element y_j by the equation as follows.

$$y_j = \sum_{i \in \mathbb{N}_I} w_{i,j} x_i + b_j, \forall j \in \mathbb{N}_O \quad (12)$$

where i, j is input and output element index and $\mathbb{N}_I, \mathbb{N}_O$, \mathbf{w} , \mathbf{b} are the number set of input and output element, the weights and biases of layers, respectively. For each fully connected layer,

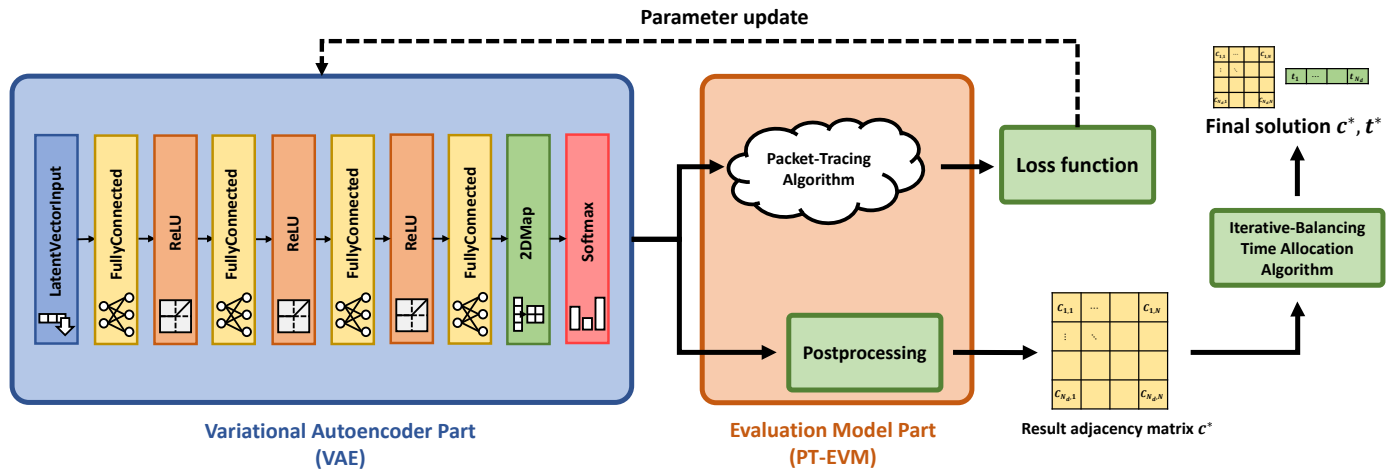


FIGURE 3. Structure flow chart of the proposed scheme to find c^* and t^*

the number of output element is set to arithmetic sequence manner, whose number of output element of last layer is fixed to $N_d(N_d + 1)$ for topology mapping (i.e., each node in \mathbb{N}_d can select the upper link among \mathbb{N}).

Between the fully connected layer, a ReLU layer is used as an activation function to provide handling on non-linear property of formulated problem. In the ReLU layer, each input element x is processed into output element y by the equation as follows.

$$y = \max(x, 0). \quad (13)$$

Next, a 2DMap layer is considered as a mean of mapping fully connected layer output to adjacency matrix form. The 2DMap layer maps the 1-Dimension input vector x totaling $N_d(N_d + 1)$ element count to N_d by $N_d + 1$ adjacency matrix, denoted as $y_{i,j}$, as follows.

$$y_{i,j} = x_{(N_d+1)(i-1)+j}, \forall i \in \mathbb{N}_d, \forall j \in \mathbb{N} \quad (14)$$

Finally, a softmax layer is applied to make the sum of row by row equal to 1, so that total outward connectivity summation for each node is equal to 1. Furthermore, the softmax layer functions as an activation function, thus enhancing the ability to handle non-linear property. The softmax layer operates for the input element x_i and the output element y_i row by row, as follows.

$$y_i = \frac{\exp x_i}{\sum_{j \in \mathbb{N}} \exp x_j}, \forall i \in \mathbb{N} \quad (15)$$

Therefore, the final autoencoder part results in an adjacency matrix c as a final output, which determines the entire topology connectivity configuration as described above.

2) PT-EVM structure

The PT-EVM part plays in a role which evaluates resulting topology from the VAE part. The right side part of Fig. 3 depicts PT-EVM structure, consists of PT algorithm module to provide achievable rate required for loss function calculation, and post-processing module to post-process inference result.

Similar to the ray-tracing algorithm, in our PT algorithm, we back-propagate and assess the achievable rate budget in backward process, starting from the packet sink. A detailed description of the procedure of our PT algorithm is as follows. Firstly, in the line 9 of Alg. 2, the focused node (i.e., a packet sink in the initial step) starts algorithm with the granted rate budget (i.e., ∞ in the initial step) given in the previous step. Next, the focused node takes its share of rate budget, R_{self} , which depends on the total inbound connection status and rate budget (line 11). We turned off auto-differentiation calculation on calculating I, B, R_{self} thus prevents affecting the assessment of the other nodes through I, B, R_{self} calculation.

Subsequently, in the line 16, the focused node give its remaining rate budget for inbound nodes. Basically, each inbound node budget is set to their link rate. However, if the remaining of the budget of focused node, $B - R_{\text{self}}$, is less than I , meaning that congestion is happening on focused node. In that case, each inbound node budget is reduced in proportion to $\frac{B - R_{\text{self}}}{I}$.

Then, the next unallocated node is called respectively in the line 19 and these steps are repeated until a termination condition (e.g., remaining allocatable rate budget drops below certain threshold, B_{th}) satisfies. This recursive algorithm spreads out through inbound connections, and the sum of all granted rate budgets over various packet-rays passes specific node implies the achievable rate of the node. With this manner of calculation, we can guarantee that all granted achievable rate could be reached into packet sink since we calculated in backward-pass from the packet sink, like in the ray of ray-tracing does.

After finalized all packet-ray backward calculation, we calculates net packet-ray for all edges of topology since a single packet-ray does not take into account other packet rays, thus net rate calculation is essential to PT-EVM modeling (line 5-7). Alg. 2 depicts implementation details of proposed packet-tracing algorithm, where I, B, R_{self} means the sum of inbound rate, the granted rate budget through packet-ray, the allocated rate of the called node, respectively. t is time slot scale factor for simulation algorithm, B_{th} is rate budget threshold for determining termination condition.

Algorithm 2 Calculation of \mathbf{R}_{sim}

```

1: main
2: global  $\mathbf{f} = \{f_i = 0 | \forall i \in \mathbb{N}_d\}$ 
3: global  $\mathbf{R} = \{R_{i,j} = 0 | \forall i \in \mathbb{N}_d, \forall j \in \mathbb{N}\}$ 
4: RatePT( $N_d + 1, \infty$ )
5:  $(\mathbf{R}_{\text{net}})_{i,j} = \text{relu}(R_{i,j} - R_{j,i}), \forall i, j \in \mathbb{N}_d$ 
6:  $(\mathbf{R}_{\text{net}})_{i,N_d+1} = R_{i,N_d+1}, \forall i \in \mathbb{N}_d$ 
7:  $(\mathbf{R}_{\text{sim}})_i = \sum_j (\mathbf{R}_{\text{net}})_{i,j}, \forall i \in \mathbb{N}_d$ 
8: end main

9: function RatePT( $n, B$ )
10: if  $B < B_{\text{th}}$ , then terminate
11:  $R_{\text{self}} = \frac{B}{1 + \sum_{j \in \mathbb{N}_d} c_{j,n}}$ 
12:  $P_j = \frac{E_j}{t}, \Gamma_{j,n} = \frac{P_j d_{j,n}^{-\alpha}}{N}, \forall j \in \mathbb{N}_d$ 
13:  $L_j = c_{j,n} t \log_2(1 + \Gamma_{j,n}), \forall j \in \mathbb{N}_d$ 
14:  $I = \sum_{j \in \mathbb{N}_d} L_j$ 
15: Turn off auto-differentiation trace on  $I, B, R_{\text{self}}$ 
16:  $R_{j,n} = L_j \min(1, \frac{B - R_{\text{self}}}{I}), \forall j \in \mathbb{N}_d$ 
17:  $f_n = 1$ 
18: for  $j \leftarrow N - \{n\}$  do
19:   if  $f_j = 0$ , then RatePT( $j, R_{j,n}$ ),  $\forall i \in \mathbb{N}_d$ 
20: end function

```

3) Training and Inferencing of the Proposed VAE Part

After we assessed each node's achievable rate through the PT-EVM part, we calculate the loss function using calculated achievable rate, and uses its value in our unsupervised learning for the VAE part. Since PT-EVM part performs auto-differentiation tracing along calculation, we can use the output of PT-EVM part into loss function calculation for the VAE part and uses it directly into a conventional neural-network training method (e.g., stochastic gradient descent). Our training of model is specific to the given topology which enables a compatibility over arbitrary node and PB configuration (e.g., the number of nodes/PBs and the positional distribution of nodes/PBs). The unsupervised learning proceeds by minimizing the loss function value L which is depicted as below:

$$L = \frac{1}{N_d} \sum_{i \in \mathbb{N}_d} (R_{\text{sim}})_i \quad (16)$$

where $(R_{\text{sim}})_i$ means node i 's rate calculated through the PT-EVM part.

Next, the parameters of the VAE part are updated towards minimizing the loss function (16) using the ADAM(Adaptive Moment Estimation) optimizing algorithm [21] which is described as below:

$$g_{t+1} \leftarrow \nabla_{\theta} L(\theta_t), \quad (17)$$

$$m_{t+1} \leftarrow \beta_1 m_t + (1 - \beta_1) g_{t+1}, \quad (18)$$

$$v_{t+1} \leftarrow \beta_2 v_t + (1 - \beta_2) g_{t+1}^2, \quad (19)$$

$$\hat{m}_{t+1} \leftarrow m_{t+1} / (1 - \beta_1^{t+1}), \quad (20)$$

$$\hat{v}_{t+1} \leftarrow v_{t+1} / (1 - \beta_2^{t+1}), \quad (21)$$

$$\theta_{t+1} \leftarrow \theta_t - \kappa \hat{m}_{t+1} / (\sqrt{\hat{v}_{t+1}} + \epsilon) \quad (22)$$

where $\theta, t, m, v, \hat{m}, \hat{v}$ are the learnable parameters (such as weights and biases in the neural network), timestep, bi-

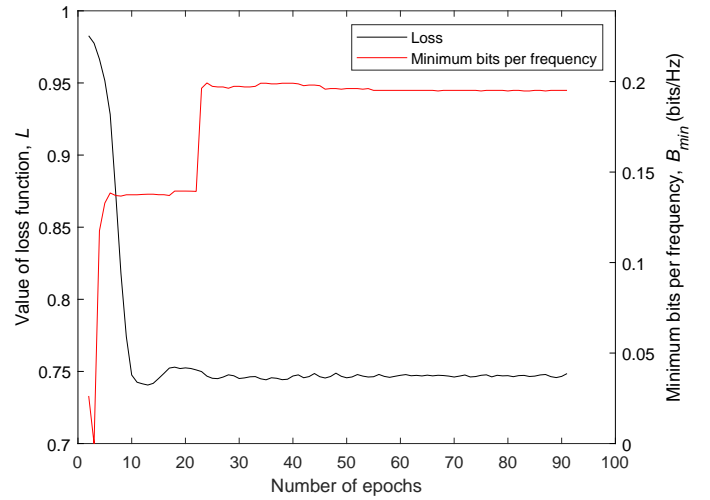


FIGURE 4. Loss and minimum bits per frequency plot on $N_d = 25, N_b = 2$ example.

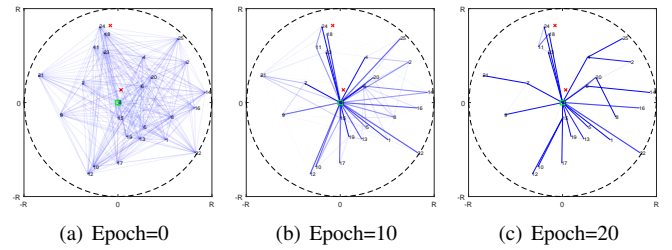


FIGURE 5. Raw topology result by epoch on $N_d = 25, N_b = 2$ example.

ased first moment, biased second raw moment, bias-corrected first moment, bias-corrected second raw moment, respectively. $\kappa, \beta_1, \beta_2, \epsilon$ are hyper-parameters for model, which means learning rate, decay rate for first moment, decay rate for second raw moment, and small scalar value used to prevent divide by zero error, respectively.

Since in [22], it has been shown that arbitrary simple prior latent vector distribution can be converted to specific target manifold distribution since first few layers of VAE structure provides such conversion appropriately. Thus, we use prior latent vector distribution as uniform distribution, $\mathcal{U}(0, 1)$, for each element during training, and measure the loss function for the sampled result.

After training, we obtain our final inference result for a specific topology by post-processing result as follows. The post-processing step finds the max index (j^*) in an adjacency matrix over row, which is defined by $C_{i,j^*} \geq C_{i,k}, \forall k \in \mathbb{N} - \{j^*\}$. Then, it zeros out other outbound connections whose connection is inferior to one which has maximum rate, satisfying the condition $C_{i,j} \in \{0, 1\}, i \in \mathbb{N}_d, j \in \mathbb{N}$. This post-processing step forces the topology result to have only one outbound connection. Such computation could be described for $i \in \mathbb{N}_d$ as below:

$$C_{i,j^*} \leftarrow 1, \quad (23)$$

$$C_{i,k} \leftarrow 0, \forall k \in \mathbb{N} - \{j^*\}. \quad (24)$$

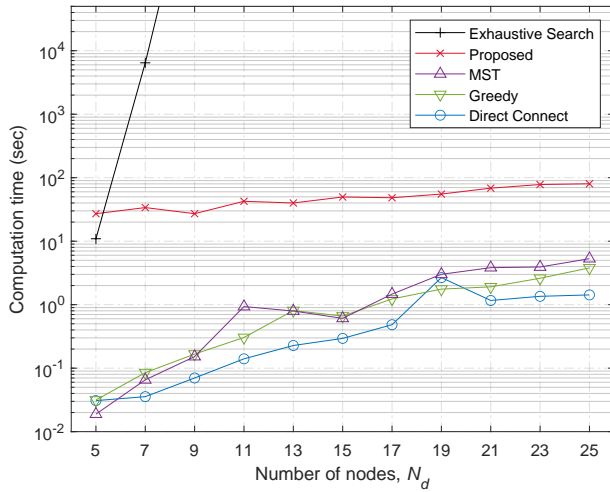


FIGURE 6. Computation time over considered schemes with respect to the number of nodes, N_d

IV. PERFORMANCE ANALYSIS AND DISCUSSIONS

We make simulations to evaluate the performance of our proposed method, of which target system model parameters are set as follows. First, path loss exponent is assumed to be $\alpha = 3$ and the bandwidth is $BW = 125$ in kHz. The noise power is defined as $N = -174 + NF + 10 \log_{10}(BW)$ in dBm, where NF is the noise figure equal to 6 dB. The nodes and PBs are distributed around a single packet sink with coverage of radius $R = 0.5$ km. Next, for the generation of wireless fading channels, $|h_{i,j}|^2$, an exponential random variable with unit mean is used. The transmit power of the PB is set to 1 W. For the energy harvesting model, the linear model is considered with $\eta = 0.7$. Finally the time frame, T is set to 100 milliseconds.

Regarding our VAE structure, we set our VAE hyper-parameters as follows. First, the learning rate is set to $\kappa = 0.001$, the decay rate for first moment is set to $\beta_1 = 0.9$, the decay rate for second raw moment is set to $\beta_2 = 0.999$, and the divide by zero prevention small scalar is set to $\epsilon = 10^{-8}$. Next, we set our VAE input vector size to $\lceil N_d \sqrt{N_d} \rceil$ and initialized our neural network weight using glorot initializer [23]. Finally, we set our neural network bias to be zero initialized. We trained our VAE neural network until the loss value smaller than previous minimum loss value has not been found for $30 + 500/N_d$ epochs.

In addition, we set PT-EVM hyper parameters as follows: time slot scale factor $t = \frac{T}{N_d}$ and rate budget threshold $B_{th} = 0.01$. Also for iterative balancing time slot allocation, we set hyper-parameters as follow: the upper bound of the difference between B_{max} and B_{min} is set to $\epsilon_1 = 10^{-6}$ bits/Hz and the minimum allocatable time slot is set to $\epsilon_2 = 10^{-7}$ sec.

For the performance comparison, we adopted 3 other conventional schemes and optimal solution cases along with our proposed scheme:

- **Optimal solution (Opt)** which exhaustively searches all cases of valid topology configuration while allocating the time slot through Algorithm 1, then choose the best rate topology.
- **Direct connect scheme (Dir)** which connects all nodes directly to the sink ($c_{n,N_d+1} = 1, \forall n \in \mathbb{N}_d$), and allocates the time slot through Algorithm 1.

- **MST scheme (MST)** which makes Minimum Spanning Tree (MST) starting from sink under initial t where $t_i = T/N_d$ for $i \in \mathbb{N}_d$, based on link costs which are set to reciprocal of the capacity, denoted as $1/(t_i \log_2(1 + \Gamma_{i,j}))$, and allocates the time slot through Algorithm 1.
- **Greedy scheme (Greedy)** which connects all nodes directly to the sink ($c_{n,N_d+1} = 1 \forall n \in \mathbb{N}_d$), and repeats randomly select node i and connect it to the one with highest achievable rate, $\min(t_i \log_2(1 + \Gamma_{i,j}), B_j), \forall j \in \mathbb{N}_d$, then allocates the time slot through Algorithm 1.
- **Proposed scheme (Prop)** which decides the topology with our proposed VAE and PT-EVM scheme and allocates the time slot with Algorithm 1.

All considered schemes are implemented on Matlab R2022b, on the computer equipped with an Intel Core i7-11700 and 16 GB of memory, without GPU acceleration.

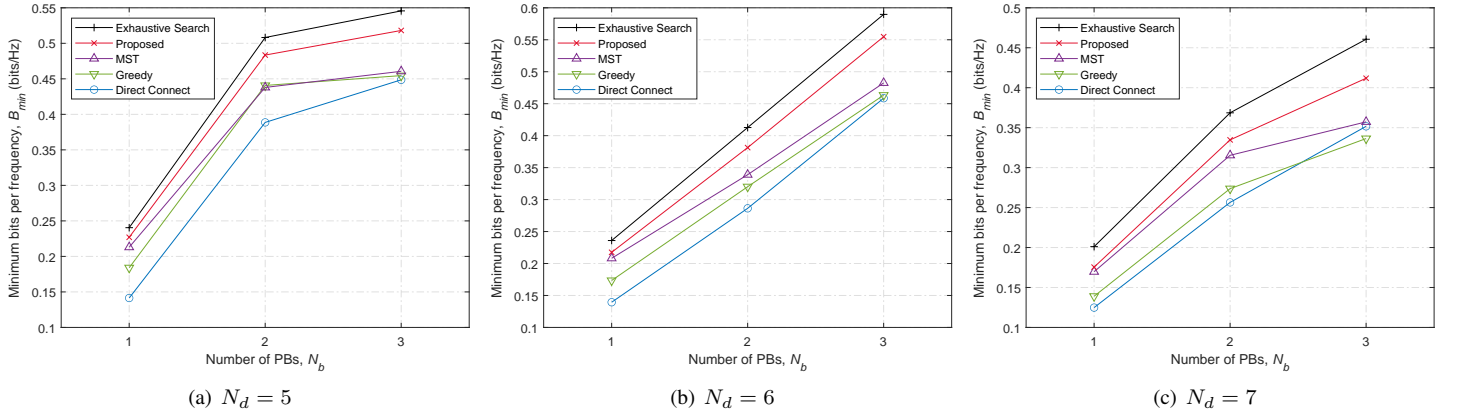
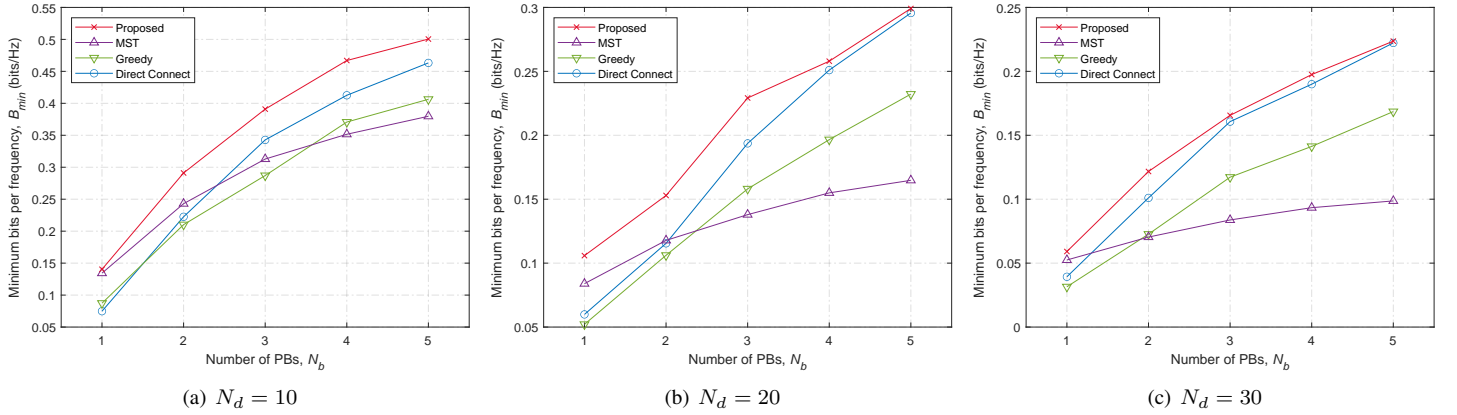
Fig. 4 shows the loss and performance (minimum bits per frequency, B_{min}) convergence with respect to the number of training epochs for the proposed VAE and PT-EVM hybrid scheme under the $N_d = 25, N_b = 2$ sample, previously described as Fig. 1. As shown in Fig. 4, the proposed VAE scheme converges to final result topology within 25 iteration(roughly take 30 seconds to compute), confirming stability of the proposed scheme.

Fig. 5 shows its resulting raw topology (not post-processed) gradually changes as learning progresses. Each subfigure shows the raw topology result in epoch 0, 10, and 20, respectively. It is visually confirmed that our proposed scheme effectively converges to a sub-optimal topology in reasonable training epoch.

Fig. 6 shows measured computation time among considered schemes with respect to the number of nodes from $N_d = 5$ to 25 with the interval of 2. Note that the number of PBs does not affect measured computation time. It is observed that the computation time of optimal solution search is growing exponentially, roughly 2 hours for $N_d = 7$ case, which makes exhaustive search method infeasible over practical environment, e.g., $N_d \geq 8$. Due to this excessive computation time, computation time of optimal solution is not suggested over $N_d \geq 8$. This fact suggests the need of alternative scheme with sub-optimal performance and rational computation time.

Although our proposed VAE and PT-EVM scheme takes more computation time over other considered schemes, the computation time gap between proposed scheme and conventional schemes are decreasing as the order of magnitude of N_d is increasing. This fact makes usage of the proposed scheme over large IoT network plausible.

Fig. 7(a) to 7(c) shows the minimum bits per frequency with respect to $N_b \in \{1, 2, 3\}$ and $N_d \in \{5, 6, 7\}$, respectively, over all considered schemes. Note that each data point on the Fig. 7(a) to 7(c) is averaged over 30 random distributions of nodes and PBs. Note that the minimum bits per frequency (bits/Hz) could be converted to a rate by multiplying $\frac{BW}{T}$, and the difference between minimum bits per frequency and maximum bits per frequency is guaranteed as below 10^{-6} bits/Hz since Alg. 1 is implemented with $\epsilon_1 = 10^{-6}$ bits/Hz. In Fig. 7(a) to 7(c), it is observed that the minimum bits per frequency increases over all considered schemes as N_b increases since the received power at each node increases. In particular,


 FIGURE 7. Performance comparison with respect to the number of PBs, N_b in $N_d \in \{5, 6, 7\}$

 FIGURE 8. Performance comparison with respect to the number of PBs, N_b in $N_d \in \{10, 20, 30\}$

MST scheme is showing relatively good performance in low power condition, while direct connect scheme is showing good performance in high power region, which means those schemes are having strengths in different power environments. On the other hand, our proposed scheme achieves the best performance than all other considered schemes at all configuration of the number of nodes and PBs, closest to the optimal solution we found.

Fig. 8(a) to 8(c) shows the minimum bits per frequency with respect to $N_b \in \{1, 2, 3, 4, 5\}$ and $N_d \in \{10, 20, 30\}$, respectively. Note that each data point on the Fig. 8(a) to 8(c) is also averaged over 30 random distributions of nodes and PBs. It is observed that the greedy method shows lower performance than direct connect method compared to fewer N_d s shown in Fig. 7(a) to 7(c), since optimal choice from a local perspective may not appropriate from a global perspective, thus deteriorates overall performance of the network. It is also confirmed that our proposed scheme is superior over three other considered schemes, ranked at the highest performance in the graph at all simulation configuration. Note that in these cases, we do not provide optimal solutions due to excessive computation time of exhaustive search. Also note that in Fig. 7(a) to 8(c), our proposed scheme is superior among various N_d from 5 to 30, showing scalability of our proposed scheme.

Therefore, we could confirm that our proposed scheme is outperforming than other existing schemes, while achieving

sub-optimal performances. Subsequently, we could infer that the performance superiority of our proposed scheme over other conventional schemes comes from these three reasons: i) The variational autoencoder stage has non-linearity property within the model, thereby can effectively cope with our NP-hard mixed integer system model problem. ii) backward-pass based evaluation stage and its novel packet-tracing algorithm gives sufficiently concise and accurate enough assessment for output topology from VAE part result at the same time, thus provides the VAE stage with an appropriate learning direction. iii) Lastly our proposed IB based time allocation algorithm fairly distributes time slot in TDMA system, which results in effective final fine-tuning on formulated max-min problem.

V. CONCLUSIONS

We formulated a max-min optimization problem for the time-division multiplexing access (TDMA) based IoT relay network. We proposed a variational autoencoder (VAE) based module to effectively solve the formulated problem, in spite of the lack of dataset and the non-linearity characteristic of problem. We also proposed the backward-pass based assessment algorithm called "Packet-Tracing" to precisely and concisely assess and train our proposed VAE module and finally proposed an iterative balancing time slot allocation algorithm to achieve TDMA fine-tuning optimization in fairness aspect. We presented the practical example of running appearance of our proposed scheme

along with the loss and performance plot, showing stability and performance of our proposed scheme. We also provided computation and performance comparison with three other conventional schemes and optimal brute-force solution. It is observed and confirmed that our proposed scheme is both stable and superior to other considered schemes through numerical simulations.

REFERENCES

- [1] K. Shafique, B. A. Khawaja, F. Sabir, S. Qazi, and M. Mustaqim, "Internet of Things (IoT) for Next-Generation Smart Systems: A Review of Current Challenges, Future Trends and Prospects for Emerging 5G-IoT Scenarios," *IEEE Access*, vol. 8, pp. 23022-23040, Feb. 2020.
- [2] B. Li, W. Wang, Q. Yin, R. Yang, Y. Li, and C. Wang, "A New Cooperative Transmission Metric in Wireless Sensor Networks to Minimize Energy Consumption per Unit Transmit Distance," *IEEE Commun. Lett.*, vol. 16, no. 5, pp. 626-628, May 2012.
- [3] D. Ma, G. Lan, M. Hassan, W. Hu, and S. K. Das, "Sensing, computing, and communications for energy harvesting IoTs: a survey," *IEEE Commun. Surveys & Tutorials*, vol. 22, no. 2, pp. 1222-1250, 2nd Quart., 2020.
- [4] F. Benkhelifa, Z. Qin, and J. A. McCann, "User Fairness in Energy Harvesting-Based LoRa Networks With Imperfect SF Orthogonality," *IEEE Trans. Commun.*, vol. 69, no. 7, pp. 4319-4334, Jul. 2021.
- [5] J.-S. Leu, T.-H. Chiang, M.-C. Yu, and K.-W. Su, "Energy Efficient Clustering Scheme for Prolonging the Lifetime of Wireless Sensor Network with Isolated Nodes," *IEEE Commun. Lett.*, vol. 19, no. 2, pp. 259-262, Dec. 2014.
- [6] T. He, K.-W. Chin, S. Soh, C. Yang, and J. Wen, "On Maximizing Min Source Rate in Power Beacon Assisted IoTs Networks," *IEEE Trans. Veh. Tech.*, vol. 69, no. 10, pp. 11880-11892, Oct. 2020.
- [7] A. Lodi, "Mixed integer programming computation," in *50 Years of Integer Programming 1958-2008*, Berlin, Germany: Springer, 2010, pp. 619-645.
- [8] C. Gambella, B. Ghaddar, and J. Naoum-Sawaya, "Optimization problems for machine learning: A survey," *European Journal of Operational Research*, vol. 290, no. 3, pp. 807-828, Aug. 2020.
- [9] H. Lee, S. H. Lee, and T. Q. S. Quek, "Deep learning for distributed optimization: applications to wireless resource management," *IEEE J. Sel. Areas Commun.*, vol. 37, no. 10, pp. 2251-2266, Oct. 2019.
- [10] J. Luo, J. Tang, D. K. C. So, G. Chen, K. Cumanan, and J. A. Chambers, "A deep-learning based approach to power minimization in multi-carrier NOMA with SWIPT," *IEEE Access*, vol. 7, pp. 17450-17460, Feb. 2019.
- [11] W. Lee, K. Lee, H. H. Choi, and V. C. M. Leung, "Deep learning for SWIPT: optimization of transmit-harvest-respond in wireless-powered interference channel," *IEEE Trans. Wireless Commun.*, vol. 20, no. 8, pp. 5018-5033, Aug. 2021.
- [12] Z. Zhang, P. Cui, and W. Zhu, "Deep learning on graphs: a survey," *IEEE Trans. on Knowledge and Data Eng.*, vol. 34, no. 1, pp. 249-270, Jan. 2022.
- [13] Y. Zhu, Y. Du, Y. Wang, Y. Xu, J. Zhang, Q. Liu, and S. Wu, "A survey on deep graph generation: Methods and applications," Dec. 2022, *arXiv:2203.06714*. [Online]. Available: <http://arxiv.org/abs/2203.06714>
- [14] D. P. Kingma and M. Welling, "Auto-encoding variational bayes," May 2014, *arXiv:1312.6114*. [Online]. Available: <http://arxiv.org/abs/1312.6114>
- [15] M. Simonovsky, and N. Komodakis, "GraphVAE: towards generation of small graphs using variational autoencoders," *International Conference on Artificial Neural Networks*, pp. 412-422, 2018.
- [16] A. Sgora, D. J. Vergados, and D. D. Vergados, "A survey of TDMA scheduling schemes in wireless multihop networks," *ACM Computing Surveys*, vol. 47, no. 3, article. 53, pp. 1-39, Apr. 2015.
- [17] S. Atapattu and J. Evans, "Optimal energy harvesting protocols for wireless relay networks," in *IEEE Trans. Wireless Commun.*, vol. 15, no. 8, pp. 5789-5803, Aug. 2016.
- [18] B. Clerckx, R. Zhang, R. Schober, D. W. K. Ng, D. I. Kim, and H. V. Poor, "Fundamentals of wireless information and power transfer: From RF energy harvester models to signal and system designs," *IEEE J. Sel. Areas Commun.*, vol. 37, no. 1, pp. 4-33, Jan. 2019.
- [19] J.-T. Lim, T. Kim, and I. Bang, "Impact of Outdated CSI on the Secure Communication in Untrusted In-Band Full-Duplex Relay Networks," *IEEE Access*, vol. 10, no. 7, pp. 19825-19835, Feb. 2022.
- [20] P. Steven, W. Martin, P. P. J. Sloan, P. Shirley, B. Smits, and C. Hansen, "Interactive ray tracing," in *ACM SIGGRAPH 2005 Courses*, pp. 119-126, 2005.
- [21] D. P. Kingma and J. Ba, "Adam: A method for stochastic optimization," Jul. 2015, *arXiv:1412.6980*. [Online]. Available: <http://arxiv.org/abs/1412.6980>
- [22] C. Doersch, "Tutorial on variational autoencoders," *arXiv:1606.05908*, Aug. 2016, [Online]. Available: <http://arxiv.org/abs/1606.05908>
- [23] X. Glorot and Y. Bengio, "Understanding the difficulty of training deep feedforward neural networks," in *Proc. 13th Int. Conf. Artif. Intell. Statist.*, pp. 249-256, 2010.



KISEOP CHUNG received the B.S degree in Electrical and Computer Engineering from Seoul National University, Seoul, South Korea, in 2022. Since June 2022, he has been a research officer at the Agency for Defense Development (ADD), South Korea. His research interests include internet of things (IoT), wireless network, unsupervised machine learning, embedded system, and hardware architecture.



JIN-TAEK LIM (S'14-M'19) received the B.S degree in Electrical and Electronic Engineering from Yonsei University, Seoul, South Korea, in 2012, and the M.S. and Ph.D. degrees in Electrical Engineering from Korea Advanced Institute of Science and Technology (KAIST), Daejeon, South Korea, in 2014 and 2019, respectively. Since March 2019, he has been a senior researcher at the Agency for Defense Development (ADD), South Korea. His research interests include internet of things (IoT), simultaneous wireless information and power transfer (SWIPT), information security, and full-duplex systems.

...